Science, Engineering and Technology Vol. 6, No. 2, pp. 190-202
www.setjournal.com https://doi.org/10.54327/set2026/v6.i2.380

Flood Inundation and Hazard Modeling Using Integrated HEC-RAS 2D and ArcGIS: A Comparative Assessment of Flood Events in the Molibagu River Watershed

Ficky Marcellino Oroh[1], Joko Nugroho[2], Olivia Maria Tumurang[1], Fiska Chintya Ezra Pangalila[1], Ronaldo Toar Palar[1], Kelvin Haryono Auwyanto[1], Misel Boro Allo[3]

[1]*Civil Engineering Department, Faculty of Engineering, Sam Ratulangi University, Manado 11480, Indonesia.*

[2]*Water Resources Engineering Research Group, Faculty of Civil and Environmental Engineering, Institut Teknologi Bandung, Bandung 40132, Indonesia.*

[3]*Civil Engineering Department, Faculty of Engineering, Universitas Tadulako, Palu 94111, Indonesia.*

Abstract

Flooding has become a major environmental issue in rapidly developing urban areas due to increasing rainfall intensity. This study develops an integrated analytical framework to analyse the relationship between rainfall variability, water discharge, flood inundation, and flood hazard modeling in the Molibagu River watershed. Hydrological analysis was conducted using thiessen polygon rainfall estimation and frequency distributions, while flood discharge was simulated using hydrologic modeling system (HEC-HMS), and river analysis was performed using a river analysis system two-dimensional (HEC-RAS 2D) approach integrated with ArcGIS software. The results indicate significant increases in rainfall intensity, peak discharge, and flood inundation extent between 2011 and 2020 across all return periods. Peak discharge for the 2-year return period increased from 44.42 m³/s to 82.42 m³/s, while flood inundation expanded from 0.531 km² to 1.257 km². Similarly, the 100-year return period showed substantial increases in both discharge and inundation extent. Spatial analysis using the hydrological hazard index (HHI) indicates a shift from low to higher hazard levels, reflecting increased flood vulnerability due to intensified hydrometeorological conditions and changing watershed conditions. These findings highlight the importance of integrated hydrological and spatial modeling to improve flood risk assessment and support effective, sustainable flood mitigation strategies.

Keywords: Molibagu River, flood inundation, HEC-RAS, ArcGIS, hydrological hazard index.

1. Introduction

Flooding is one of the most destructive natural hazards affecting tropical watersheds, causing substantial environmental, economic, and social impacts worldwide [1]. Among these hazards, flooding is a highly destructive natural phenomenon, consistently causing significant human and economic losses annually, with a tendency for increasing intensity [2]. Therefore, monitoring the level of vulnerability and resilience to flooding has become increasingly crucial [3]. In this context, evaluating and strengthening major urban centers is essential to increase their resilience [4]. Furthermore, identifying and assessing the vulnerability of these areas to various risks and threats is a key prerequisite for achieving effective resilience [5]. Flooding in urban areas is now one of the most serious environmental problems facing rapidly

Corresponding author: Misel Boro Allo (misel.boroallo@gmail.com)
Received: 30 May 2026; Revised: 6 September 2026; Accepted: 14 September 2026; Published: 25 September 2026

growing cities, particularly in arid and very arid regions. This situation is further exacerbated by the increase in extreme hydrological events due to global warming, changing rainfall patterns, and accelerated urbanization [6]. The increasing intensity of global climate change has contributed to increasing human and economic losses from natural disasters [7]. The proximity of river channels to populated areas increases the risk level, including a higher frequency of flooding and potential erosion of riverbanks [8]. Flooding is a global and ongoing threat to the environment, infrastructure, and human safety and life [9]. Meteorological factors, duration, and spatial distribution of rainfall, have a direct influence on sediment availability and the synchronization between runoff and sediment transport into the channel [10]. Abdessamed et al. [11] developed a Hydrologic Engineering Center–Hydrologic Modeling System (HEC-HMS) based hydrological model followed by flood simulations on a river network, where the flow geometry was previously defined through cross-sections using Hydrologic Engineering Center–River Analysis System (HEC-RAS) 1D (one-dimensional). Peker et al. [12] generated flood hazard maps using HEC-HMS and HEC-RAS integrated into a GIS (Geographic Information System) environment for the Göksu River basin. Ennouini et al. [13] also conducted rainfall-based flood simulations in a hydrological network using rainfall hyetographs for various return periods. Therefore, the results of flood simulation models can only be considered highly reliable if the analysis is carried out professionally, utilizing efficient and integrated data acquisition and computational algorithms [14]. Flood studies have commonly focused on hydrological analysis, hydraulic simulation, or flood inundation mapping separately, without comprehensively integrating rainfall variability, flood discharge, inundation extent, and hydrological hazard assessment into a unified framework. However, limited studies have quantitatively evaluated how changes in hydrometeorological conditions and watershed characteristics simultaneously affect flood dynamics and hazard evolution over different periods, particularly in tropical river basins. Existing studies rarely quantify how hydrometeorological variability and land-use changes jointly influence temporal changes in flood dynamics and vulnerability patterns. Furthermore, studies integrating hydrological–hydraulic modeling and GIS-based hazard assessment remain limited in tropical Indonesian watersheds, where rapid land-use changes and increasing rainfall variability may significantly alter flood characteristics over time. In addition, most studies in tropical Indonesian watersheds still rely on conventional one-dimensional (1D) approaches and lack temporal comparative analysis to evaluate the impacts of land-use change and increasing extreme rainfall intensity on flood vulnerability. Although 1D hydraulic models have been widely used because of their computational efficiency and simplicity, these approaches often have limitations in representing complex floodplain flow behavior and spatial inundation characteristics. Such limitations may reduce the accuracy of flood representation in areas with varying topographic conditions and dynamic hydrological responses. Moreover, increasing urban expansion and changes in land cover conditions may alter runoff generation and flow patterns, leading to significant changes in flood extent and hazard levels. Understanding these temporal changes is essential for identifying shifts in flood-prone areas and improving flood risk management strategies. Therefore, a more integrated analytical approach is needed to provide a comprehensive understanding of the interactions among hydrometeorological conditions, watershed dynamics, and flood impacts.

Therefore, this study proposes an integrated hydrological–hydraulic–spatial modeling framework to assess temporal changes in flood inundation and hydrological hazard levels in the Molibagu River watershed between 2011 and 2020. Specifically, this study aims to analyze changes in rainfall variability and annual discharge characteristics and evaluate their influence on flood inundation extent and hazard levels. The novelty of this study lies in the integration of temporal flood comparison and GIS-based hydrological hazard indexing by combining HEC-HMS, HEC-RAS 2D (two dimensional), ArcGIS, and the Hydrological Hazard Index (HHI) within a single analytical framework. This integration enables the assessment of the entire flood response chain, from rainfall variability and watershed runoff generation to hydraulic inundation patterns and spatial hazard classification. Unlike previous approaches that commonly assess hydrological response, hydraulic behavior, or flood mapping independently, the proposed framework links these components to provide a more comprehensive evaluation of temporal flood hazard changes. The findings are expected to improve flood risk assessment and support sustainable flood mitigation planning and watershed management in tropical river basins.

2. Methodology

2.1. Study Area

The Molibagu River is geographically located at approximately 0°24′36.34″ N and 123°58′50.32″ E, with a main river channel length of about 14.75 km and a watershed area of approximately 50.58 km². Climatologically, the region is characterized by a tropical climate, with average annual temperatures ranging from 20 to 30°C and annual rainfall between 1000-1500 mm. Figure 1 shows the location of the study area and the geographical extent of the watershed. The watershed exhibits diverse topographic conditions, ranging from flat lowlands to hilly terrains; about 25% of the area is classified as flat to gently undulating, while around 40% consists of undulating to hilly landscapes, indicating a clear morphological transition from downstream to upstream areas. The Molibagu River watershed is dominated by volcanic soils (72.08%), followed by alluvial (14.33%) and karst soils (13.58%). Forest cover occupies 23.85 km², while the built-up area increased from 0.61 km² in 2011 to 1.05 km² in 2020. These variations contribute to significant differences in stream power, particularly in the upstream sections, thereby enhancing both vertical and lateral erosion processes. Moreover, the variability in rainfall plays a crucial role in influencing river discharge dynamics and sediment transport within the watershed, as periods of heavy rain can increase runoff and sediment flow, whereas dry periods tend to decrease both.

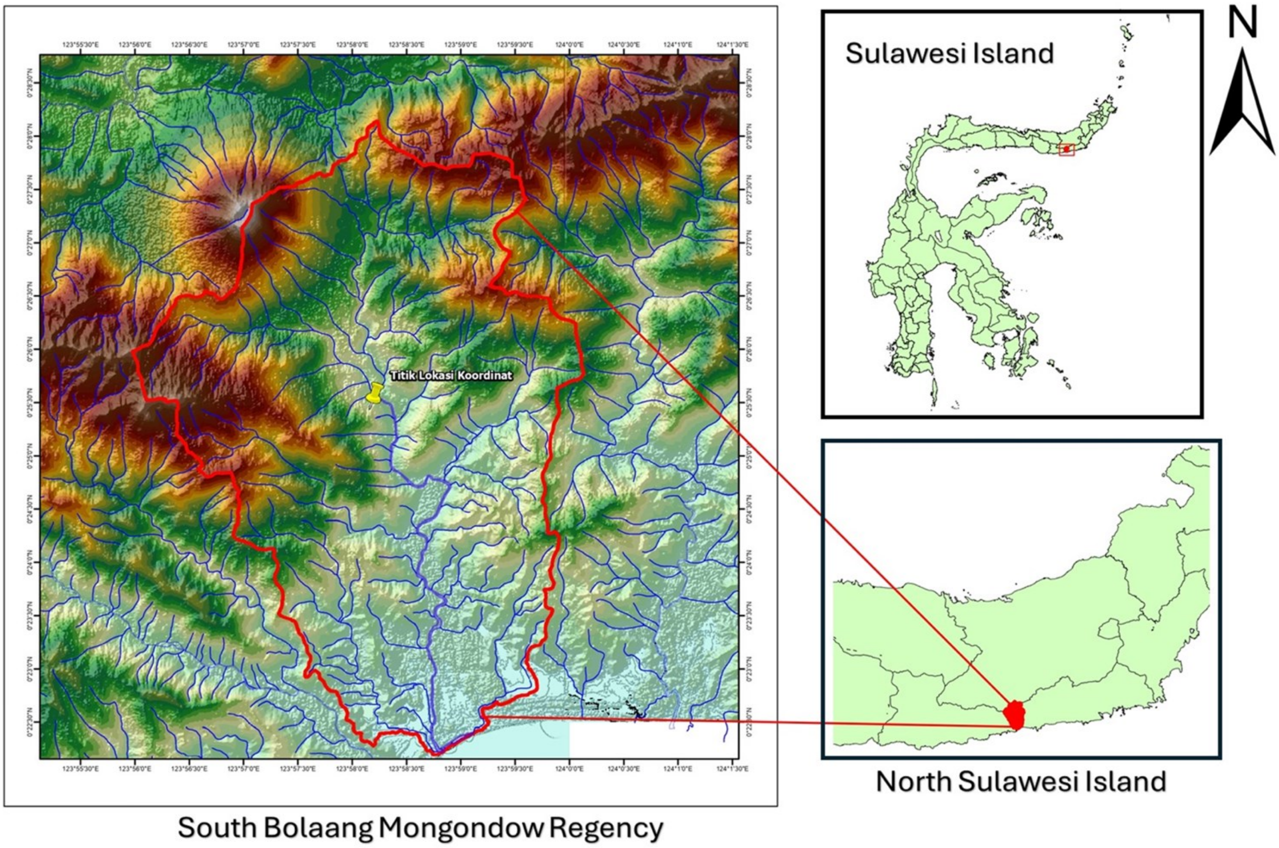

Figure 1. Study area and sampling locations in the Molibagu River watershed.

2.2. Data Collection and Calculation

The selection of 2011 and 2020 was primarily determined by the availability of complete and comparable datasets required for the flood analysis, including rainfall and land-use data. The year 2011 was treated as the baseline, while 2020 represented the most recent period for which consistent input data were available. Data collection and processing in this study were conducted in the Molibagu River, which covers the Bolaang Uki District, covering 12 villages (Matayangan, Sondano, Tolondadu II, Molibagu, Salongo, West Salongo, Pinolantungan, Soguo, Popodu, East Salongo, Toluaya, and Pintadia). Figure 2 shows the Molibagu River basin.

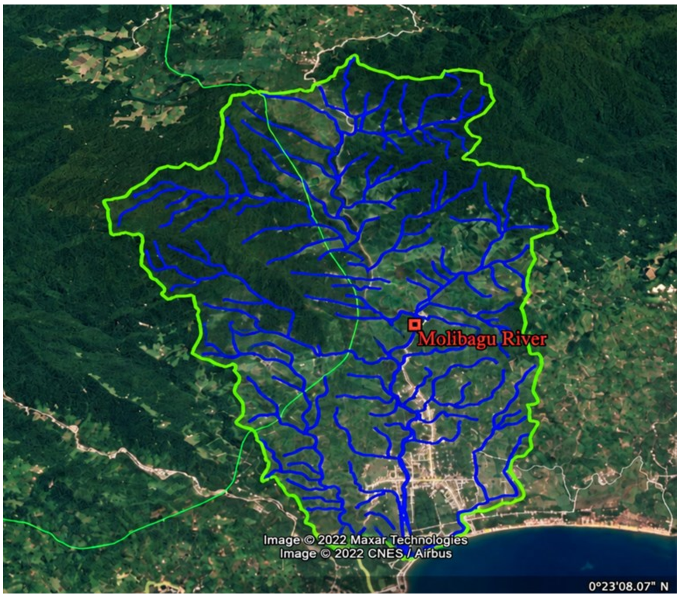

Figure 2. Molibagu River Basin.

The datasets utilized include hydrological, topographic, and river characteristic data, which were systematically processed to support hydrological and hydraulic modeling. Average areal rainfall was estimated using the Thiessen polygon method based on data from two available hydrological stations to represent the spatial distribution of precipitation across the study area. Rainfall frequency analysis was performed using several statistical distributions, including Log-Normal [15], Log-Pearson Type III [15], and Gumbel [16], followed by goodness-of-fit evaluation using the chi-square test to identify the most appropriate distribution model. Furthermore, the SCS – CN (Soil Conservation Service – Curve Number) method [17] is used to model land use-based rainfall–runoff transformation as a basis for estimating flood discharge. Hydrological modeling was conducted using HEC-HMS [18], while flood hydraulic simulations were carried out using a two-dimensional (2D) approach in HEC-RAS [19], integrated with spatial analysis in ArcGIS to generate flood inundation maps [20]. The two-dimensional computational domain in HEC-RAS covered an area of approximately 50.58 km² and was discretized using a uniform mesh with a cell size of 20 × 20 m. The mesh resolution was selected by considering the spatial resolution of the DEMNAS (Indonesian National Digital Elevation Model) data, the relatively simple morphological characteristics of the Molibagu watershed, and the balance between spatial representation and computational efficiency. Local mesh refinement was not applied because the modeled river reach does not contain complex hydraulic features, such as bridges, weirs, river bifurcations, or flood-control structures, that would require a finer mesh resolution. The upstream boundary condition was defined using discharge hydrographs generated by the calibrated HEC-HMS model for flood return periods of 2, 5, 10, 25, 50, and 100 years. These hydrographs were applied as unsteady-flow inputs at the upstream boundary of the HEC-RAS 2D computational domain. At the downstream boundary, a normal-depth boundary condition was specified based on the riverbed slope near the watershed outlet. Observed discharge data covering five years were used to evaluate the HEC-HMS model. The 2011 flood event was used for model calibration, whereas the 2020 flood event was used for validation. Model performance was evaluated using the Nash–Sutcliffe Efficiency (NSE) [21], root mean square error (RMSE) [21], coefficient of determination (R^2) [21], and the relative difference between the simulated and observed peak discharges. Manning’s roughness coefficients were assigned based on channel characteristics and land-cover conditions. Values of 0.035, 0.045, 0.030, and 0.080 were applied to the main river channel, agricultural areas, settlements, and forests, respectively, following standard hydraulic roughness classifications. The Curve Number (CN) method was employed within the HEC-HMS loss model to represent watershed runoff characteristics based on land use and hydrologic soil group conditions. The CN values were determined from land use classification and hydrologic soil group analysis, while the watershed retention parameter was estimated from the CN value, as expressed in Eq. (1). Higher CN values indicate lower infiltration capacity and greater runoff potential.

$$S = \frac{25400 - 254CN}{CN} \quad (1)$$

where: S is the potential maximum retention (mm), and CN is the curve number ranging from 0 to 100, representing watershed characteristics associated with land use, soil type, and hydrological conditions.

The Hydrological Hazard Index (HHI) was developed by integrating several spatial parameters influencing flood hazard levels, including slope, land use, soil type, rainfall, topography, distance from rivers, flood inundation extent, and flood depth. An equal-weighting approach was applied to all parameters. This approach was selected because the parameters represent distinct components of flood generation, propagation, and hydraulic response. Equal weighting was therefore used to minimize subjective bias and prevent any single parameter from disproportionately influencing the final HHI. The hydrological hazard index (HHI) values were subsequently classified into low, moderate, and high hazard categories using the class interval method based on the cumulative scores derived from all spatial parameters. The composite HHI scores were then classified into three hazard levels: low ($140 \leq$ HHI < 310), moderate ($310 \leq$ HHI < 440), and high ($440 \leq$ HHI ≤ 640). Each parameter was assigned a score according to its relative contribution to flood hazard potential, and the HHI value was calculated by summing the weighted scores of all parameters, as expressed in Eq. (2). The resulting HHI values were subsequently classified into low, moderate, and high hazard categories using the class interval method, as expressed in Eq. (3).

$$\mathrm{HHI} = \sum_{i=1}^{n} Xi \quad (2)$$

$$\mathrm{I} = \frac{\mathrm{HHI(max)} - \mathrm{HHI(min)}}{\mathrm{k}} \quad (3)$$

where: HHI is hydrological hazard index, Xi is the score of parameters i, and I is the class interval.

3. Result and Discussion

3.1. Model Validation, Model Uncertainty and Limitations

Table 1 summarizes the statistical performance of the HEC-HMS model. The calibration and validation results showed high NSE and R^2 values and low RMSE values, indicating good agreement between the simulated and observed discharges.

Table 1. Statistical performance of the HEC-HMS model (5-year return period).

Parameter	2011	2020
Simulated Peak Discharge (m^3/s)	101.16	189.63
Observed Peak Discharge (m^3/s)	98.86	185.17
NSE	0.891	0.912
RMSE (m^3/s)	0.312	0.286
Relative peak-discharge difference (%)	2.33	2.41
R^2	0.931	0.957

For the 2011 calibration event, the simulated and observed peak discharges were 101.16 and 98.86 m^3/s, respectively, corresponding to a relative difference of 2.33%. For the 2020 validation event, the simulated and observed peak discharges were 189.63 and 185.17 m^3/s, respectively, with a relative difference of 2.41%. The mean relative difference was approximately 2.37%, indicating that the model reproduced the observed peak discharges reasonably well. The model results should nevertheless be interpreted by considering several sources of uncertainty. Rainfall input is considered the principal model forcing because rainfall intensity, duration, and spatial and temporal distribution directly influence runoff volume, peak discharge, and hydrograph timing. Uncertainty in rainfall input may propagate from the HEC-HMS simulation into the HEC-RAS 2D results and consequently affect the simulated flood depth, velocity, inundation extent, and hazard classification. Therefore, the simulated flood inundation extent, and hydrological hazard index should be regarded as model-based estimates rather than exact values. The Wilcoxon signed-rank test indicated that the increase in simulated peak discharge between 2011 and 2020 was statistically significant, with the p-value equal to 0.031.

3.2. Rainfall intensity and flood discharge

Figure 3 shows the distribution of rainfall based on return periods. The percentage increase in rainfall intensity from 2011 to 2020 for return periods of 2, 5, 10, 25, 50, and 100 years was 15.62%, 25.25%, 29.01%, 32.31%, 34.10%, and 35.55%, respectively. This study indicates a consistent increasing trend in rainfall and peak discharge across all return periods.

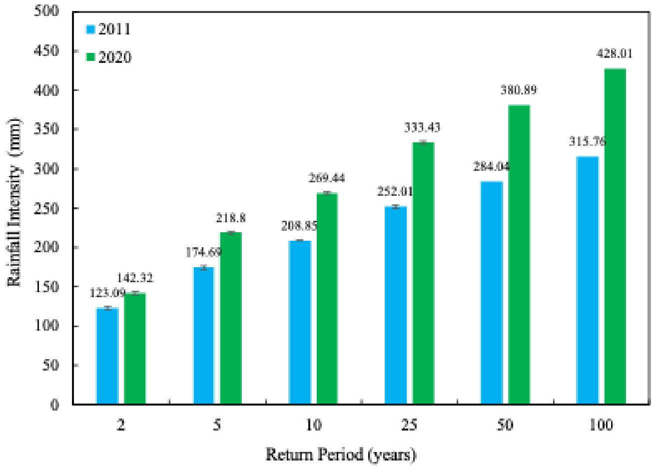

Figure 3. Rainfall Intensity.

Figure 4 shows the distribution of peak discharge based on return periods, indicating a significant increase from 2011 to 2020 for the return periods of 2, 5, 10, 25, 50, and 100 years, with percentage increases of approximately 85.55%, 87.46%, 83.92%, 84.79%, 85.16%, and 85.41%, respectively. This finding indicates an increase in watershed runoff response and the potential for increasingly extreme flood events over time. This phenomenon reflects changes in the characteristics of the hydrological response (hydrological performance), which is mainly influenced by increasing intensity of extreme rainfall events. This combination of factors contributes to increased surface runoff while accelerating the hydrological response at the watershed scale. Furthermore, a more significant increase at a larger return period indicates that extreme events experience a stronger intensification compared to events with higher frequency. This indicates a shift in rainfall and flood discharge distribution toward more extreme conditions, which directly increases the potential and risk of flooding in river basins. The observed increase in rainfall intensity and peak discharge is consistent with previous studies indicating that rainfall variability and hydrometeorological conditions significantly affect watershed hydrological responses. Similar findings were reported by Peker et al. [12], who demonstrated that the integration of HEC-HMS, HEC-RAS, and GIS revealed increasing flood susceptibility under intensified hydrometeorological conditions. From an environmental perspective, this trend has implications for increased soil erosion rates, sediment accumulation in river bodies, and decreased water quality due to increased sediment transport. Potential further impacts include disruption of ecosystem balance, including changes in vegetation structure and degradation of natural habitats, which can ultimately worsen the stability of the overall hydrological system.

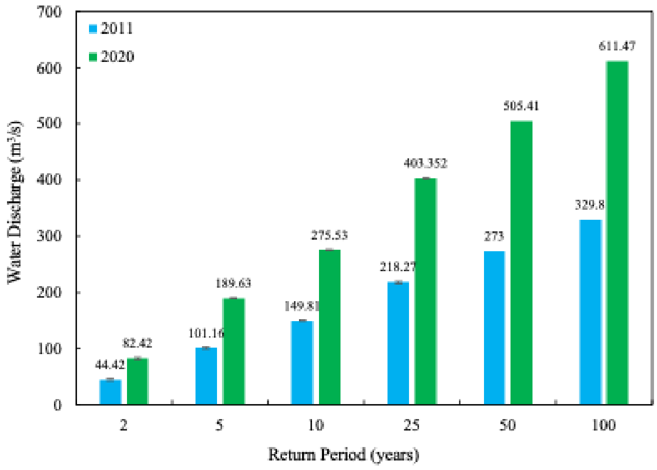

Figure 4. Water Discharge.

3.3. Hydrograph

Table 2 presents a comparison of inflow discharge hydrographs between 2011 and 2020 for different return periods. The results indicate a substantial increase in peak discharge magnitude over time. For the 2-year return period, the peak discharge increased from 44.42 m^3/s in 2011 to 82.42 m^3/s in 2020, (representing an increase of approximately 85.55%). Similarly, for the 100-year return period, the peak discharge increased from 329.8 m^3/s to 611.47 m^3/s, (corresponding to an increase of approximately 85.41%). Although both periods exhibit relatively similar hydrograph shapes, with peak discharge occurring between the 4th until 6th hour, the 2020 response is notably more rapid and sustained, as reflected by a steeper rising limb and a longer duration of elevated discharge. The Curve Number (CN) values were determined based on land use classification and hydrologic soil group analysis. The weighted CN values increased slightly from 42.04 in 2011 to 42.20 in 2020, associated with changes in watershed characteristics and hydrological response within the Molibagu watershed. These patterns suggest a decline in the watershed's retention and infiltration capacity, leading to a greater proportion of rainfall being converted into surface runoff. The accelerated watershed response observed in 2020 indicates a reduction in infiltration and storage capacity, resulting in a shorter lag time and a faster conversion of rainfall into surface runoff. Similar hydrological behavior was also reported by Zhang et al. [22] who observed that watersheds experiencing intensified rainfall and changing watershed conditions exhibited reduced infiltration capacity and accelerated surface runoff generation This shift can be conceptually associated with land-use changes, particularly the conversion of vegetated areas into built-up or open land, which reduces the soil's capacity to store and infiltrate water. In addition, hydrometeorological factors, such as increased intensity of extreme rainfall events, further amplify the speed and magnitude of the hydrological response. The combined influence of anthropogenic and climatic drivers thus contributes to higher peak discharges, especially under longer return periods. Consequently, the observed increase in peak discharge and the acceleration of watershed response time are likely to elevate flood risk in terms of both frequency and severity. These findings highlight the need for more adaptive watershed management strategies, including stricter control of land-use change, enhancement of infiltration capacity through soil and water conservation measures, and the implementation of improved drainage systems alongside ecosystem-based flood mitigation approaches.

Table 2. Inflow Discharge.

Time (h)	**Inflow Discharge (m^3/s)**											
	2011						2020					
	2 years	5 years	10 years	25 years	50 years	100 years	2 years	5 years	10 years	25 years	50 years	100 years
1	1.82	1.9	1.97	2.05	2.14	2.22	1.94	2.02	2.1	2.18	2.27	2.36
2	8.4	18.9	27.8	40.1	50.2	60.3	15.6	36.2	52.7	77.1	96.6	116.8
3	18.6	42.5	63.1	91.8	114.9	138.7	35.8	81.5	118.4	173.4	217.3	262.9
4	32.8	74.8	110.7	161.3	201.7	243.8	60.3	138.4	201.2	294.5	360	430
5	44.42	94.8	139.5	199.2	245.6	292	82.42	177.8	257.8	369.5	469.8	561.5
6	41.8	101.16	149.81	218.27	264.8	319.5	77.6	189.63	275.53	403.35	494.2	592.3
7	35.6	93.2	145.6	211.3	272.96	329.8	66.8	176.8	272.6	398.5	505.42	611.47
8	29.6	80.5	132	192.4	255.3	312.6	57.8	158.8	244.3	365.2	485.1	586
9	24.4	68.7	113.4	166	227.4	281.8	49.6	139.5	214.9	322.4	440.6	531.2
10	20.1	57.9	95.7	140.2	191.3	237.2	42.6	120.3	185.9	279.4	392.5	473.4
11	16.6	47.7	79.1	117	159.3	197.6	36.4	103.2	159.8	240.6	338.8	409.2
12	13.7	39.2	65.2	96.5	131.6	163.5	30.9	88	136.8	205.8	291.6	352.1
13	11.3	32.2	53.5	79.4	107.9	134.3	26.1	74.9	117.3	176.6	250.7	302
14	9.4	26.4	43.8	65.2	88.6	110.1	21.9	63.9	99.7	150.9	214.8	259.1
15	7.8	21.7	35.9	53.5	72.8	90.3	18.3	54.1	84.4	128.8	184.9	222.5
16	6.5	17.8	29.5	44.1	60	74.4	15.3	45.9	71.2	109.8	158.8	190.7
17	5.4	14.6	24.2	36.3	49.3	61.2	12.8	38.8	60.2	93.7	135.7	162.8
18	4.6	12.1	20	30	40.8	50.7	10.8	32.8	50.9	79.9	115.7	138.9
19	3.9	10	16.5	24.9	33.9	42.1	9.1	27.8	43.2	68.1	98.6	118.3
20	3.4	8.3	13.8	20.8	28.3	35.2	7.7	23.7	36.8	58.1	84	100.9
21	3	6.9	11.6	17.5	23.8	29.6	6.5	20.2	31.4	49.8	71.3	85.7
22	2.7	5.8	9.8	14.8	20.1	25	5.5	17.2	26.9	42.6	60.7	72.9
23	2.5	4.9	8.3	12.6	17.1	21.2	4.7	14.7	23	36.6	51.8	62.2
24	2.3	4.2	7.1	10.7	14.5	18	3.9	12.5	19.7	31.4	44.3	53.2
25	2.1	3.6	6	9.1	12.2	15.2	2.3	10.4	16.7	25.8	36.2	43.6

3.4. Flood Inundation

Table 3 presents the results of hydraulic simulations using HEC-RAS to evaluate changes in flood inundation extent based on conditions in 2011 and 2020. The simulation results indicate a substantial increase in flooded areas across both return periods. For the 2-year return period, the inundation area expanded from 0.531 km² in 2011 to 1.257 km² in 2020, (representing an increase of approximately 136.7%). Similarly, for the 100-year return period, the flooded area increased from 1.609 km² to 2.282 km², (corresponding to an increase of about 41.8%). Overall, the modeling results for both years and return periods consistently show an increasing trend in both inundation extent and water depth. For the two-year return period, flooding in 2011 was relatively confined to the river channel with limited lateral spread.

Table 3. Flood inundation areas between 2011 and 2020.

Return Period	Flooded Area 2011 (km^2)	Flooded Area 2020 (km^2)
2-year	0.531	1.257
100-year	1.609	2.282

The spatial distribution of flood inundation under the selected return periods is presented in Figures 5 and 6. However, in 2020, a noticeable expansion of the inundation area occurred, indicating a change in the watershed's hydrological response. In contrast, during the 100-year return period, floodwaters extended more extensively into floodplains and adjacent areas, accompanied by greater depths and a more uniform spatial distribution.

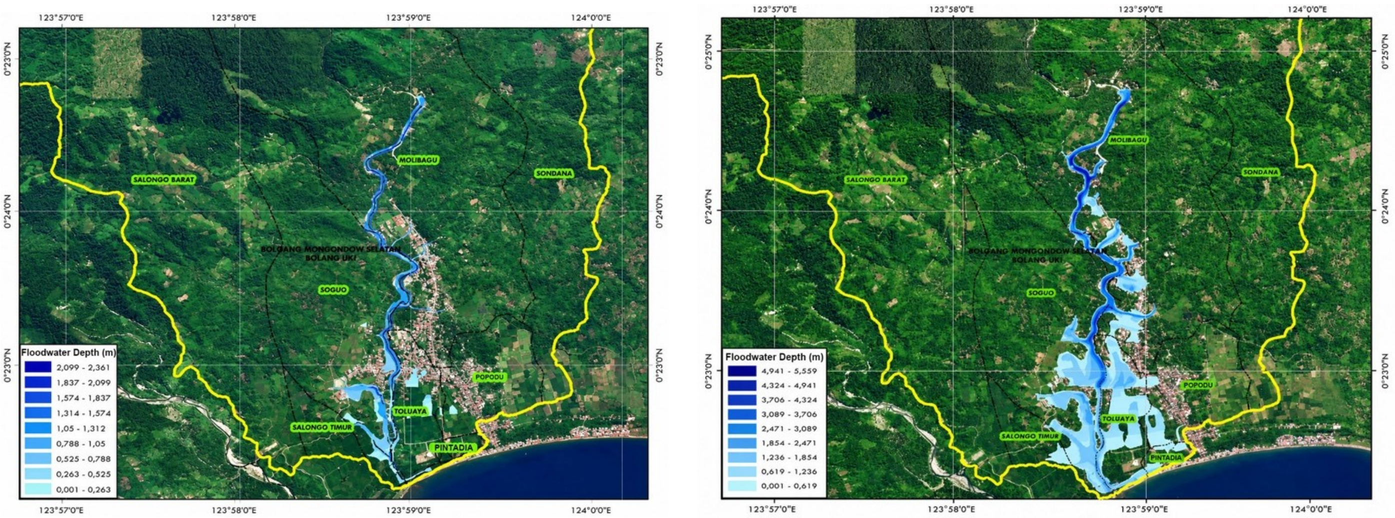

Figure 5. Floodwater Depth 2011, (a) 2-year return period, (b) 100-year return period.

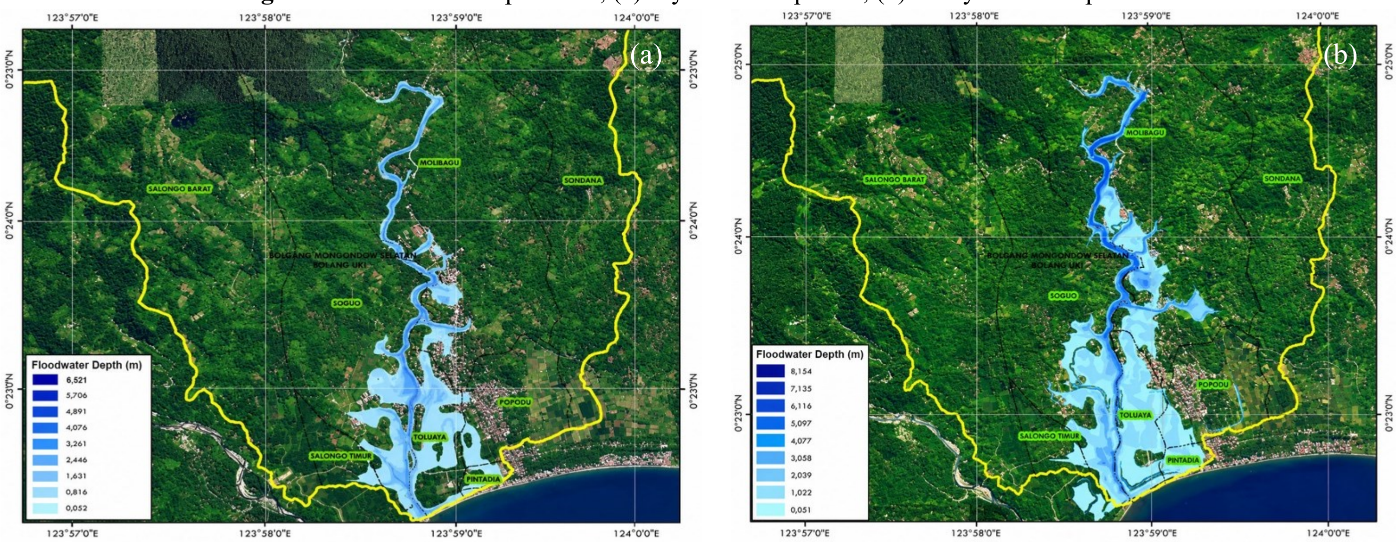

Figure 6. Floodwater Depth 2020, (a) 2-year return period, (b) 100-year return period.

The increase in flood inundation extent is consistent with studies showing that intensified rainfall and watershed alteration significantly increase flood-prone areas. Similar observations were reported by Desalegn et al. [23] and Khan et al. [24] who found that hydrodynamic simulations in small catchments demonstrated increased flood hazard under changing rainfall conditions. These interannual differences are influenced not only by variations in discharge magnitude associated with return periods but also by changes in the watershed's physical and hydrological characteristics. Increased surface runoff generated by intensified rainfall and watershed response, together with diminished river storage capacity that may be associated with sedimentation or channel narrowing, could have contributed to the intensified flooding. These findings highlight a degradation in the watershed's hydrological and hydraulic functions between 2011 and 2020, as reflected in the increased flood extent and depth, even under lower return periods. Consequently, this trend indicates a significant rise in flood vulnerability, which calls for integrated mitigation strategies, including improved river management, stricter land-use regulation, and risk-based spatial planning to reduce future flood impacts.

The spatial distribution of flood inundation under the selected return periods is presented in Figures 5 and 6. The similarity between the 2020 2-year inundation area and the 2011 100-year inundation area has important implications for flood risk management. It suggests that flood conditions previously associated with rare extreme events may now occur much more frequently. Consequently, existing drainage systems, river channels, embankments, and other flood-control structures designed using historical conditions may no longer provide adequate protection. Flood risk management should therefore include the revision of hazard maps and hydraulic design standards, stricter control of development in downstream floodplains and river corridors, improvement of drainage and river conveyance capacity, and protection of upstream infiltration areas. In addition, early-warning systems, evacuation planning, and community preparedness should be strengthened to address the increasing frequency and extent of flooding.

3.5. Hydrological Hazard Index (HHI)

Figure 7 presents a hydrological hazard map and a detailed spatial overview of flood vulnerability levels in the Molibagu City area. This map categorizes the study area into three hazard categories: low, moderate, and high providing a more comprehensive understanding of the spatial distribution of flood risks. Zones with high hazard levels are generally located in lowlands, close to rivers, and in urban areas with impermeable surfaces and limited drainage capacity. These conditions contribute to the increased potential for water accumulation during high-intensity rainfall events. The map was compiled using ArcGIS software through an overlay process using the Union method, which integrates all spatial layers into the smallest polygon units with complete attributes. A normalization step was carried out to standardize eight main parameters, including slope, land use, soil type, rainfall, topography, distance from rivers, flood inundation extent, and flood depth, and combine them into a single integrated index, namely the Hydrological Hazard Index (HHI). Next, the continuous HHI raster values were reclassified into three hazard classes to facilitate interpretation and quantitative analysis.

The proportion of each hazard class is presented in Table 4. The results indicate a substantial shift in flood hazard distribution between 2011 and 2020. The low hazard category decreased from 93.8% to 71.7%, representing a reduction of 22.1% in low-risk areas. In contrast, the moderate hazard category increased by 18.6%, from 5.7% in 2011 to 24.3% in 2020. Similarly, the high hazard category increased from 0.5% to 4.0%, corresponding to an increase of 3.5%. These changes indicate a spatial expansion of moderate and high flood hazard zones and reflect increasing flood susceptibility within the Molibagu watershed over time.

Table 4. Area Distribution of Hydrological Hazard in the Study Area.

Description	HHI Map	Area Proportion 2011	Area Proportion 2020
Low Hazard	Green	93.8%	71.7%
Moderate Hazard	Yellow	5.7%	24.3%
High Hazard	Red	0.5%	4.0%

In 2011, areas with high to very high vulnerability were limited and concentrated along major river corridors and downstream areas near the coast, while most river basins were dominated by low vulnerability levels. However, in 2020, there was a significant expansion of areas with moderate to high vulnerability, which not only followed river flow patterns but also extended to floodplains and downstream residential areas. The spatial expansion of moderate and high-hazard zones suggests increasing flood vulnerability and declining watershed resilience over time. GIS-based flood hazard mapping has been widely recognized as an effective tool for supporting risk-based spatial planning and flood mitigation policies. Similar findings were reported by Peker et al. [12], who demonstrated that the integration of hydrological and hydraulic modeling with GIS techniques can effectively identify flood-prone areas and improve flood risk assessments. The expansion of areas with moderate to high hazard categories reflects an increase in the frequency and intensity of potential inundation, indicating a decline in the environment's capacity to control surface runoff. This change is thought to be influenced by increasing rainfall intensity together with watershed characteristics, reduced soil infiltration capacity, sedimentation that decreases river conveyance capacity, and localized expansion of built-up areas, all of which contribute to higher flood hazard. Furthermore, hydrometeorological factors, particularly increased rainfall intensity, also play a role in increasing flood risk. Overall, a comparison between conditions in 2011 and 2020 shows a trend toward increasing flood vulnerability, characterized by the expansion of high-risk areas and an increased potential impact on areas previously considered relatively safe. The spatial pattern of flood hazard shows that moderate- and high-hazard zones are concentrated in the downstream part of the Molibagu watershed, particularly along the main river corridor and in the areas surrounding Popodu, Pintadia, and Salongo. In 2011, these zones were relatively narrow and mainly confined to areas immediately adjacent to the river. By 2020, the moderate-hazard zone had expanded considerably toward the eastern and southeastern floodplain, while the high-hazard zone became more extensive and spatially continuous along the lower river and coastal area. These conditions promote flow accumulation and increase the likelihood of prolonged flooding. In contrast, the upper and central parts of the watershed remained predominantly within the low-hazard category because of their higher elevation, steeper terrain, and greater distance from the main river channel. The observed expansion between 2011 and 2020 therefore indicates an increasing concentration of flood hazard in the downstream floodplain, where topographic, hydraulic, and land-surface conditions interact to intensify flood susceptibility.

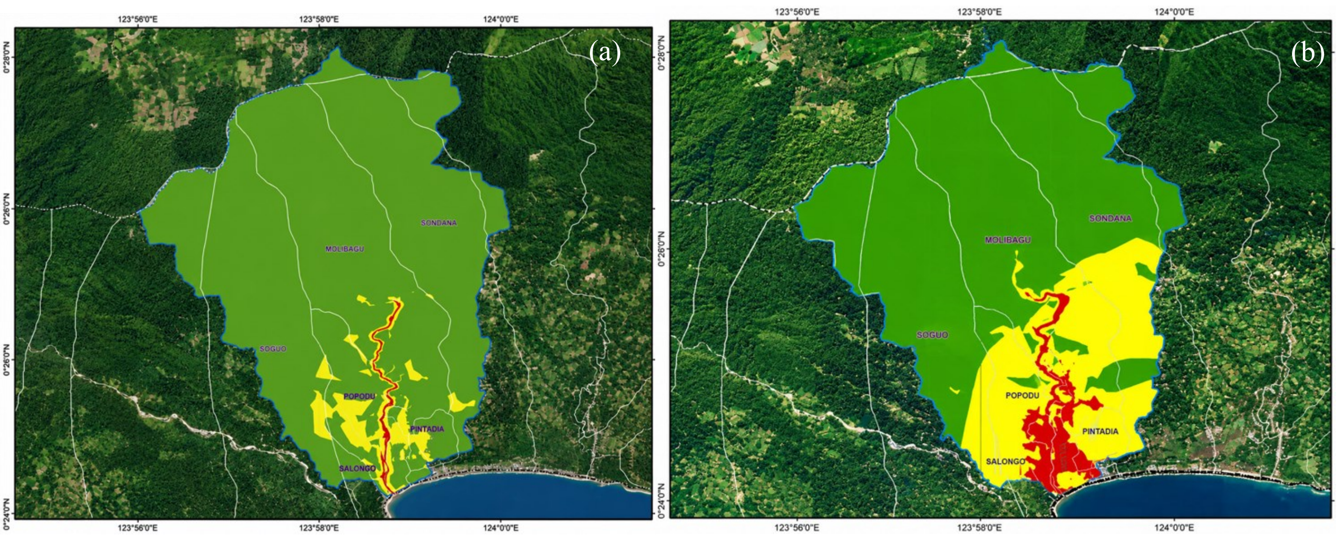

Figure 7. Spatial distribution of hydrological hazard levels in the Molibagu watershed for (a) 2011 and (b) 2020.

The findings of this study are consistent with those of Supratman et al. [25] who reported that urban expansion and vegetation loss in the tropical Mampang watershed increased peak discharge by approximately 10% and intensified the level of flood hazard. However, their analysis focused on a highly urbanized lowland watershed and a single 25-year return-period scenario, whereas the present study evaluated the Molibagu watershed under six return periods ranging from 2 to 100 years. These consistent findings indicate that land-use change can intensify flood responses in tropical watersheds, although the magnitude and spatial distribution of the impacts may vary according to watershed morphology, soil characteristics, and channel capacity. These findings may assist local governments in developing evidence-based flood management policies through the implementation of risk-based land-use planning, improved drainage infrastructure, river channel maintenance, and ecosystem-based mitigation measures. In addition, the flood hazard maps generated in this study can support decision-making processes related to zoning regulations, flood early warning systems, and the prioritization of mitigation programs in highly vulnerable areas.

4. Conclusion

This study developed an integrated hydrological–hydraulic–spatial modeling framework by combining HEC-HMS, HEC-RAS 2D, and GIS-based analysis to assess flood inundation and hydrological hazard dynamics in the Molibagu River watershed. The results demonstrated a significant increase in rainfall intensity and peak discharge from 2011 to 2020 across all return periods, indicating an intensification of hydrometeorological conditions within the watershed. Consequently, flood inundation areas expanded substantially, particularly in lowland and densely populated regions, reflecting the increasing vulnerability of the study area to extreme flood events. The hydrological hazard index (HHI) analysis further revealed a spatial transition from predominantly low-hazard zones in 2011 toward moderate and high-hazard categories in 2020. This trend indicates a decline in watershed resilience, which may be associated with intensified rainfall conditions and changes in watershed hydrological response, potentially leading to increased surface runoff and greater flood susceptibility. The integration of temporal flood comparison with GIS-based hazard assessment represents the main contribution of this study and provides a more comprehensive understanding of flood dynamics in tropical river basins. Overall, the proposed framework offers a reliable approach for flood risk assessment and supports evidence-based decision-making for sustainable watershed management and flood mitigation planning. This study has several limitations. The hydrological analysis was based on rainfall data from only two rainfall stations, which may not fully represent the spatial variability of precipitation across the watershed. This study did not explicitly consider sedimentation processes or the effects of climate change, which may influence river-channel capacity, peak discharge, and flood-inundation patterns. Local stakeholders should strengthen land-use control, protect vegetated and riparian areas, improve flood monitoring, and conduct regular river maintenance in vulnerable locations. Future research should incorporate climate change scenarios and sediment transport analysis to improve the reliability of flood assessment in the Molibagu watershed.

Competing Interests Statement

The authors declare no known competing financial interests or personal relationships that could have influenced the work reported in this paper.

Data Availability Statement

All data generated or analyzed during this study are included in this published article. Additional information related to the study may be made available by the corresponding author or first author upon reasonable request at misel.boroallo@gmail.com or fickyoroh19@unsrat.ac.id.

Funding Statement

No external funding: The authors received no specific funding for this research.

Statement on the Ethical Use of AI Tools

AI-assisted tools were used only for language refinement and grammatical improvement during the preparation of the manuscript. All technical content, analysis, interpretations, and conclusions were developed and verified by the authors.

Author Contribution Roles

Ficky Marcellino Oroh: Software, Validation, Data Curation, Visualization, and Writing Original Draft.
Joko Nugroho : Supervision, Software, Validation, Data Curation, and Visualization
Olivia Maria Tumurang: Data Curation, Visualization and Validation.
Fiska Chintya Ezra Pangalila: Methodology, Formal analysis, and Investigation.
Ronaldo Toar Palar: Methodology, Investigation and Formal analysis.
Kelvin Haryono Auwyanto: Validation, Data Curation, and Visualization
Misel Boro Allo: Software, Validation, Visualization, Writing – original draft and Writing – review and editing.

Acknowledgments

The authors acknowledge the assistance of colleagues and reviewers whose comments contributed to improving the quality of this manuscript.

References

[1] H. Ma *et al.*, "Amplification of downstream flood stage due to damming of fine-grained rivers," *Nat. Commun.*, vol. 13, no. 1, p. 3054, 2022, doi: 10.1038/s41467-022-30730-9.
[2] J. Zhang, S. Wang, J. Huang, Y. He, and Y. Ren, "The Precipitation-Recycling Process Enhanced Extreme Precipitation in Xinjiang, China," *Geophys. Res. Lett.*, vol. 50, no. 15, p. e2023GL104324, Aug. 2023, doi: 10.1029/2023GL104324.
[3] Y. Zhao, J. Li, Y. Tian, and J. Li, "Distinguishing Extreme Precipitation Mechanisms Associated with Atmospheric Rivers and Nonatmospheric Rivers in the Lower Yangtze River Basin," *J. Clim.*, vol. 37, no. 15, pp. 3995–4010, 2024, doi: 10.1175/JCLI-D-23-0400.1.
[4] R. Li *et al.*, "Effects of urbanization on the water cycle in the Shiyang River basin: based on a stable isotope method," *Hydrol. Earth Syst. Sci.*, vol. 27, no. 24, pp. 4437–4452, 2023, doi: 10.5194/hess-27-4437-2023.
[5] D. Di *et al.*, "A CFD-DEM investigation into hydraulic transport and retardation response characteristics of drainage pipeline siltation using intelligent model," *Tunnelling and Underground Space Technology*, vol. 152, p. 105964, 2024, doi: 10.1016/j.tust.2024.105964.
[6] H. El Naggar and H. Abdelrazik, "Assessing community awareness for flood disasters in the UAE through human-centered design," *International Journal of Disaster Risk Reduction*, vol. 107, p. 104475, 2024, doi: 10.1016/j.ijdrr.2024.104475.
[7] R. Clasing, E. Muñoz, J. L. Arumí, and V. Parra, "Remote Sensing with UAVs for Flood Modeling: A Validation with Actual Flood Records," *Water (Basel).*, vol. 15, no. 21, Art. no. 3813, 2023, doi: 10.3390/w15213813.
[8] B. R. Pandey, H. Knoblauch, and G. Zenz, "Potential Dam Breach Flood Assessment with the 2D Diffusion and Full Dynamic Wave Equations Using a Hydrologic Engineering Center-River Analysis System," *Water (Basel).*, vol. 16, no. 2, pp. 1–24, 2024, doi: 10.3390/w16020277.
[9] S. Ghimire, "Application of a 2D Hydrodynamic Model for Assessing Flood Risk from Extreme Storm Events," *Climate*, vol. 1, no. 3, pp. 148–162, 2013, doi: 10.3390/cli1030148.
[10] Y. Long *et al.*, "Suspended sediment-discharge hysteresis characteristics and controlling factors in a small watershed of southern China," *Catena (Amst).*, vol. 243, p. 108198, 2024, doi: 10.1016/j.catena.2024.108198.
[11] D. Abdessamed and B. Abderrazak, "Coupling HEC-RAS and HEC-HMS in rainfall–runoff modeling and evaluating floodplain inundation maps in arid environments: case study of Ain Sefra city, Ksour Mountain. SW of Algeria," *Environ. Earth Sci.*, vol. 78, no. 19, p. 586, 2019, doi: 10.1007/s12665-019-8604-6.
[12] İ. B. Peker, S. Gülbaz, V. Demir, O. Orhan, and N. Beden, "Integration of HEC-RAS and HEC-HMS with GIS in Flood Modeling and Flood Hazard Mapping," *Sustainability (Switzerland)*, vol. 16, no. 3, Art. no. 1226, Feb. 2024, doi: 10.3390/su16031226.
[13] W. Ennouini, A. Fenocchi, G. Petaccia, E. Persi, and S. Sibilla, "A complete methodology to assess hydraulic risk in small ungauged catchments based on HEC-RAS 2D Rain-On-Grid simulations," *Natural Hazards*, vol. 120, no. 8, pp. 7381–7409, 2024, doi: 10.1007/s11069-024-06515-2.
[14] V. Kumar, K. V. Sharma, T. Caloiero, D. J. Mehta, and K. Singh, "Comprehensive Overview of Flood Modeling Approaches: A Review of Recent Advances," *Hydrology*, vol. 10, no. 7, Art. no. 141, 2023, doi: 10.3390/hydrology10070141.
[15] A. I. Shah and N. Das Pan, "Evaluation of probability distribution methods for flood frequency analysis in the Jhelum Basin of North-Western Himalayas, India,"

Cleaner Water, vol. 2, p. 100044, 2024, doi: 10.1016/j.clwat.2024.100044.

[16] S. Doiphode and V. Swami, "Rainfall analysis and deriving design storm for hydrological modelling of Koyna dam catchment area in Maharashtra state of India," *J. Environ. Manage.*, vol. 359, p. 121082, 2024, doi: 10.1016/j.jenvman.2024.121082.

[17] J. An *et al.*, "Scenario-dependent responses of soil conservation service flow to climate change across karst development gradients in the Pearl River Basin," *Ecol. Indic.*, vol. 185, p. 114758, 2026, doi: 10.1016/j.ecolind.2026.114758.

[18] C. Mo *et al.*, "Simulation of flood processes under extreme precipitation scenarios based on an improved HEC-HMS model in a typical karst mountainous basin, southwest China," *J. Hydrol. (Amst).*, vol. 669, p. 135154, 2026, doi: 10.1016/j.jhydrol.2026.135154.

[19] G. M. Munna, M. J. Bin Alam, M. M. Uddin, N. Islam, A. A. Orthee, and K. Hasan, "Runoff prediction of Surma basin by curve number (CN) method using ARC-GIS and HEC-RAS," *Environmental and Sustainability Indicators*, vol. 11, p. 100129, 2021, doi: 10.1016/j.indic.2021.100129.

[20] S. Hazra, K. S. Bora, and P. A. Singh, "Mapping World: A Comparative Analysis of Functionality and Usability between QGIS and ArcGIS," *Recent Advances in Computer Science and Communications*, vol. 18, no. 4, article ID e266625583325292025, doi: 10.2174/0126662558332529240919063643.

[21] S. Ullah *et al.*, "Evaluating land use and climate change impacts on Ravi river flows using GIS and hydrological modeling approach," *Sci. Rep.*, vol. 14, no. 1, p. 22080, 2024, doi: 10.1038/s41598-024-73355-2.

[22] P. Zhang *et al.*, "Rainfall-runoff generation patterns and key influencing factors in the plain of the Taihu Lake Basin, China," *J. Hydrol. Reg. Stud.*, vol. 58, p. 102247, 2025, doi: 10.1016/j.ejrh.2025.102247.

[23] H. Desalegn and A. Mulu, "Mapping flood inundation areas using GIS and HEC-RAS model at Fetam River, Upper Abbay Basin, Ethiopia," *Sci. Afr.*, vol. 12, p. e00834, 2021, doi: 10.1016/j.sciaf.2021.e00834.

[24] S. Khan *et al.*, "Climate-driven flood hazard assessment in data-scarce mountainous basins using a GIS-based machine learning and hydrodynamic modelling under CMIP6 SSP scenarios," *Sci. Rep.*, vol. 16, no. 1, p. 1800, 2026, doi: 10.1038/s41598-025-31390-7.

[25] M. Supratman, M. S. B. Kusuma, M. Cahyono, and A. A. Kuntoro, "Flood Hazard Assessment Due to Changes in Land Use and Cover," *Civil Engineering Journal (Iran)*, vol. 10, no. 12, pp. 3874–3891, Dec. 2024, doi: 10.28991/CEJ-2024-010-12-04.